Phase Characterization and Properties of Completely Saturated Quaternary Phosphonium Salts. Ordered, Room-Temperature Ionic Liquids

Hui Chen,[†] Dylan C. Kwait,[†] Z. Serpil Gönen,[‡] Brian T. Weslowski,[§] David J. Abdallah,[†,||] and Richard G. Weiss*,[†]

Department of Chemistry, Georgetown University, Washington, D.C. 20057-1227, Department of Chemistry, University of Maryland, College Park, Maryland 20742, and George Mason University, Fairfax, Virginia 22030

Received October 25, 2001. Revised Manuscript Received August 13, 2002

The properties of four completely saturated and one partially saturated salts consisting of methyl-tri-*n*-decylphosphonium cations and either chloride, chloride monohydrate, bromide, bromide monohydrate, or nitrate anions are reported. Their neat phase behavior has been examined by polarizing optical microscopy, differential scanning calorimetry, and X-ray diffraction. The monohydrates form smectic phases that persist in >90 °C ranges and extend from below room temperature; they are ordered, room-temperature ionic liquid crystals. The nitrate salt becomes liquid-crystalline above room temperature and the other two salts remain as soft solids to their isotropization temperatures. The locations of two solvatochromic dyes, Nile Red and 1,1-dicyano-2-[6-(dimethylamino)naphthylen-2-yl]propene, within the ionic assemblies have been approximated from UV/vis absorption and fluorescence spectra, and the temperature (phase) dependence of the conductivities and dielectric constants of some of the salts have been measured. Some comparisons with properties of isotropic, room-temperature ionic liquids are made.

Introduction

Ionic liquids have received a great deal of attention recently due to their broad range of potential uses.[1] A combination of negligible vapor pressure, high ionic conductivity, and thermal stability make many ionic liquids[2] effective "green solvents" for environmentally friendly applications.[3] The most common ionic liquid crystals (i.e., ionic liquids with some long-range molecular order) are *N*,*N*-dialkylimidazolium or *N*-alkylpyridinium salts.[4,5] A wide range of polymeric ionic liquid crystals[6] as well as liquid-crystalline ionic liquids comprised of quaternary ammonium and phosphonium salts with long alkyl chains[7−13] are known also. However, solid−liquid crystal transitions of all of the latter occur at superambient temperatures.

* To whom correspondence should be addressed. E-mail: weissr@georgetown.edu.
[†] Georgetown University.
[‡] University of Maryland.
[§] George Mason University.
[||] Current address: Agere Systems, 9333 S. John Young Parkway, Orlando, FL 32819.

(1) (a) Blanchard, L. A.; Hancu, D.; Bechman, E. J.; Brennecke, J. F. *Nature* **1999**, *399*, 28. (b) Suarez, P. A. Z.; Einloft, S.; Dullius, J. E. L.; de Souza, R. F.; Dupont, J. *J. Chim. Phys.* **1998**, *95*, 1626. (c) Gordon, C. M.; Holbrey, J. D.; Kennedy, A. R.; Seddon K. R. *J. Mater. Chem.* **1998**, *8*, 2627. (d) Huddleston, J. G.; Willauer, H. D.; Swatloski, R. P.; Visser, A. E.; Rogers, R. D. *Chem. Commun.* **1998**, 1765. (e) Wasserscheid, P.; Keim, W. *Angew. Chem., Int. Ed.* **2000**, *39*, 3772. (f) Welton, T. *Chem. Rev.* **1999**, *99*, 2071. (g) Gordon, C. M.; McLean, A. J. *Chem. Commun.* **2000**, 1395. (h) Earle, M. J.; McCormac, P. B.; Seddon, K. R. *Green Chem.* **1999**, *1*, 23. (i) Cull, J. D.; Holbrey, J. D.; Vargas-Mora, V.; Seddon, K. R.; Lye, G. J. *Biotechnol. Bioeng.* **2000**, *69*, 227. (j) Laali, K. K.; Gettwert, V. J. *J. Org. Chem.* **2001**, *66*, 35. (k) Visser, A. E.; Swatloski, R. P.; Rogers, R. D. *Green Chem.* **2000**, *2*, 1. (l) Liu, F.; Abrams, M. B.; Baker, R. T.; Tumas, W. *Chem. Commun.* **2001**, 433. (m) Carmichael, A. J.; Haddleton, D. M.; Bon, S. A. F.; Seddon, K. R. *Chem. Commun.* **2000**, 1237. (n) Owens, G. S.; Abu-Omar, M. M. *Chem. Commun.* **2000**, 1165. (o) Brown, R. A.; Pollet, P.; McKoon, C. A.; Liotta, C. L.; Jessop, P. G. *J. Am. Chem. Soc.* **2001**, *123*, 1254. (p) Baker, S. N.; Baker, G. A.; Kane, M. A.; Bright, F. V. *J. Phys. Chem. B* **2001**, *105*, 9663. (q) Reynolds, J. L.; Erdner, K. R.; Jones, P. B. *Org. Lett.* **2002**, *4*, 917. (r) Fletcher, K. A.; Pandey, S.; Storey, I. K.; Hendricks, A. E.; Pandey, S. *Anal. Chim. Acta* **2002**, *453*, 89. (s) Hagiwara, R.; Hirashige, T.; Tsuda, T.; Ito, Y. *J. Electrochem. Soc.* **2002**, *149*, D1.

(2) Carmichael, A. J.; Hardacre, C.; Holbrey, J. D.; Nieuwenhuyzen, M.; Seddon, K. R. *Proc. Electrochem. Soc.* **2000**, *99-41*, 209.

(3) Earle, M. J.; Seddon, K. R. *Pure Appl. Chem.* **2000**, *72*, 1391.

(4) (a) Cull, S. G.; Holbrey, J. D.; Vargas-Mora, V.; Seddon, K. R.; Lye, G. J. *Biotechnol. Bioeng.* **2000**, *69*, 227 (b) Chauvin, Y.; Mussmann, L.; Olivier, H. *Angew. Chem., Int. Ed. Engl.* **1995**, *34*, 2698. (c) Earle, M. J.; McCormac, P. B.; Seddon, K. R. *Chem. Commun.* **1998**, 2245. (d) Carmichael, A. J.; Earle, M. J.; Holbrey, J. D.; McCormac, P. B.; Seddon, K. R. *Org. Lett.* **1999**, *1*, 997.

(5) (a) Holbrey, J. D.; Seddon, K. R. *J. Chem. Soc., Dalton Trans.* **1999**, 2133. (b) Gordon, C. M.; Holbrey, J. D.; Kennedy, A. R.; Seddon, K. R. *J. Mater. Chem.* **1998**, *8*, 2627. (c) Lee, C. K.; Huang, H. W.; Lin, I. J. B. *Chem. Commun.* **2000**, 1911.

(6) Masson, P.; Guillon, D. *Mol. Cryst. Liq. Cryst.* **2001**, *362*, 313, and refs therein.

(7) (a) Lee, Y. S.; Sujadi, D.; Rathman, J. F. *Langmuir* **1996**, *12*, 6202. (b) Kokkinia, A.; Paleos, C. M. *Mol. Cryst. Liq. Cryst.* **1990**, *186*, 239. (c) Arkas, M.; Tsiourvas, D.; Paleos, C. M.; Skoulios, A. *Chem. Eur. J.* **1999**, *5*, 3202. (d) Margomenou-Leonidopoulou, G. *ICTAC News* **1993**, *26*, 24. (e) Tschierske, C. *J. Mater. Chem.* **1998**, *8*, 1485. (f) Tschierske, C. *Prog. Polym. Sci.* **1996**, *21*, 775. (g) Przedmojski, J.; Dynarowicz-Latka, P. *Phase Trans.* **1999**, *70*, 1333. (h) Terreros, A.; Galera Gomez, P. A.; Lopez Cabarcos, E.; Müller, A. *Colloids Surf. A* **2000**, *164*, 47. (i) Fosse, N.; Brohan, L. *Mol. Cryst. Liq. Cryst.* **1999**, *330*, 129. (j) Fuller, S.; Shinde, N. N.; Tiddy, G. J. T. *Langmuir* **1996**, *12*, 1117. (k) Paleos, C.; Arkas, M.; Seghrouchni, R.; Skoulios, A. *Mol. Cryst. Liq. Cryst.* **1995**, *268*, 179.

(8) Kunitake, T.; Okahata, Y. *J. Am. Chem. Soc.* **1977**, *99*, 3860.

(9) Israelachvili, J. N.; Mitchell, D. J.; Ninham, B. W. *J. Chem. Soc., Faraday Trans 2* **1976**, *272*, 1525.

(10) Abdallah, D. J.; Bachman, R. E.; Perlstein, J.; Weiss, R. G. *J. Phys. Chem. B* **1999**, *103*, 9269.

10.1021/cm010930x CCC: $22.00
Published on Web 09/24/2002

Here, we report the structures and properties of what are (to the best of our knowledge) the first completely saturated, room-temperature, *ordered* ionic fluids: methyl-tri-*n*-decylphosphonium cations with chloride monohydrate or bromide monohydrate as anions.[14] The nitrate salt (whose anion is unsaturated) becomes liquid-crystalline above room temperature and the anhydrous chloride and bromide salts remain as soft solids below their isotropization temperatures. In another work, we have studied alkyl-tri-*n*-alkylphosphonium salts (**nPmA**; where **n** is the length of the fourth short *n*-alkyl chain, **m** is the length of the three long *n*-alkyl chains, and **A** is the anion) extensively because they are generally more thermally stable and exhibit wider liquid-crystalline ranges and lower onset temperatures than their nitrogen analogues.[15]

Results and Discussion

General Considerations. The packing arrangements of the **nPmA** salts in their solid phases are determined, in large part, by the length of the *n*-alkyl chains and the nature of the anions. Usually, the solid → liquid-crystal transition temperature is lowest and the range of liquid crystallinity is broadest when **n** = 1.[15] Additionally, previous studies have revealed that when **n** and **A** are unchanged, the range of liquid crystallinity increases and the onset temperature of the liquid-crystalline phase decreases when **m** is decreased (18 → 14 → 10).[15] However, if **m** is very short, as in the case of **1P4Br**, an isotropic liquid is found at room temperature and no liquid crystallinity is evident at lower temperatures.

Some previously examined **1PmNO$_3$** and **1PmBr** salts exhibit bilayer smectic A phases (SmA_2) that commence above room temperature.[15] The respective solid → SmA_2 (T_{K-SmA2}) and SmA_2 → isotropic (T_{SmA2-I}) phase transition temperatures of the longer chained nitrates are 69.4 and 107.8 °C (**1P18NO$_3$**) and 43.4 and 110.4 °C (**1P14NO$_3$**). The chlorides, **1P18Cl** (mp 95.5−97.5 °C) and **1P14Cl** (mp 105.0−105.5 °C), form only highly birefringent, deformable solid phases. Other **1P10A** salts prepared previously either are not liquid-crystalline (**1P10ClO$_4$** and **1P10PF$_6$**) or possess a narrow range of liquid crystallinity (30−50 °C for **1P10BF$_4$**).

Optical Microscopy, Thermal Gravimetry, and Differential Scanning Calorimetry. Thermal gravimetric analyses (TGA) showed a 3.7% and 2.8% continuous weight loss between room temperature and ≈120 °C from hydrated **1P10Cl** (**1P10Cl·H$_2$O**) and hydrated **1P10Br** (**1P10Br·H$_2$O**), respectively, corresponding to the removal of about one water molecule (3.4% and 3.2% calculated for loss of one water per **1P10Cl·H$_2$O** and **1P10Br·H$_2$O**). The weight loss was continuous rather than abrupt because water molecules are loosely held and not well-ordered within the liquid-crystalline phases. Their slow loss entails a change in composition as well as a phase change. Thus, loss of a water molecule at one site affects the molecular organization at neighboring sites. Consistent with it being virtually anhydrous and much less deliquescent than **1P10Cl** or **1P10Br**, an aliquot of **1P10NO$_3$** that had been exposed to the air showed minimal weight changes (<0.6%) when heated from room temperature to 140 °C.

Table 1. Phase Transition Temperatures from DSC and Optical Microscopy (in Parentheses) and Heats of Transition (Δ*H*)

		cooling		heating	
	transition[a]	T[b] (°C)	$-\Delta H$ (kJ/mol)	T[b] (°C)	ΔH (kJ/mol)
1P10NO$_3$[c]	K−K	−36.8	0.8	−10.0	11.4
	K−LC	62.1	1.5	59.7	1.7
	LC−I	83.8	2.7	82.5 (74.4−76.2)	2.9
1P10Br[d]	K−K	*f*	*f*	3.8	13.6
	K−I	96.7	8.2	95.2 (97.5−99.5)	9.4
1P10Br·H$_2$O[d,h]	K−K	*f*	*f*	−9.2	4.0
	K−LC	*f*	*f*	−3.8	9.7
	LC−I	96.8	1.0	94.8	2.5
1P10Cl·H$_2$O[e,h,i]	K−K	−19.7	4.9	−16.7	3.8
	K-LC	*f*	*f*	7.6	5.8
	LC−I	101.8	2.1	102.7	1.5
1P10Cl[g]	K−K	−20.0	4.2	−20.1	−0.4
	K−K	*f*	*f*	8.0	7.9
	K−I	101.0	9.9	98.9 (96.2−97.9)	10.5

[a] K = solid, LC = liquid crystal, I = isotropic. [b] From peak onsets. [c] Heated first to isotropic temperature and then cooled. [d] Cooled from ambient temperature and then heated. [e] Second cooling and heating; see text. [f] Obscured from detection by a false peak created when dry ice coolant was added near room temperature. [g] Fourth cooling and heating; see text. [h] Data for LC−I transitions were obtained by heating the samples from 47 to 120 °C at 10 °C/min and then cooling; other transition temperatures were determined by heating at 5 °C/min. [i] Data for the K−LC transition was obtained by cooling the sample to −10 °C and then heating it to 40 °C at 10 °C/min.

Phase transition temperatures determined by optical microscopy and differential scanning calorimetry (DSC) were nearly the same (Table 1). When heated, all of the salts except **1P10NO$_3$** possess remarkably similar (subambient) onset temperatures and ranges (90−110 °C) for the phases immediately preceding the transitions to the isotropic phase (at ≲100 °C). The reproducibility of the second and subsequent DSC heating scans, taken to >120 °C, demonstrates the thermal stability of all the anhydrous salts; exotherms from cooling scans were detected for all of the endotherms in the heating scans except as noted. The salts decompose when heated to ≈300 °C (DSC).

Because the hydrates lose their water molecules at much lower temperatures, the reversibility of their transitions could not be ascertained. The first DSC cooling and heating thermogram (recorded in that order starting at room temperature) of a sample of **1P10Cl·H$_2$O** exhibited very broad peaks at −0.8 °C (cooling) and at 25.1 °C (heating) not observed in subsequent thermograms. The second and third cooling and heating cycles were from a partially hydrated salt; the fourth and subsequent cycles indicated complete loss of water

(11) Kanazawa, A.; Tsutsumi, O.; Ikeda, T.; Nagase, Y. *J. Am. Chem. Soc.* **1997**, *119*, 7670
(12) (a) Lu, L.; Weiss, R. G. *Chem. Commun.* **1996**, 2030. (b) Lu, L.; Weiss, R. G. *Langmuir* **1995**, *11*, 3630.
(13) Lu, L.; Sharma, N.; Nagana Gowda, G. A.; Khetrapal, C. L.; Weiss, R. G. *Liq. Cryst.* **1997**, *22*, 23.
(14) The iodide, **1P10I**, was synthesized and found to be liquid-crystalline at room temperature, but no details are reported here because elemental analyses were unsatisfactory.
(15) Abdallah, D. J.; Robertson, A.; Hsu, H.-F.; Weiss, R. G. *J. Am. Chem. Soc.* **2000**, *122*, 3053.

(i.e., formation of **1P10Cl**; see Supporting Information). A heating exotherm from **1P10Cl**, tentatively ascribed to a glass → crystal transition, is shifted to lower temperatures as the runs are repeated. The DSC curves of **1P10Br·H_2O** follow the same trends; the third heating curve was almost the same as that of **1P10Br**.

A solid−solid transition was detected at ≈37 °C in the DSC thermograms of **1P10Cl**, but only during the first heating scan. Subsequent scans were reproducible, but lacked this feature. A solid → LC transition is observed at ≈60 °C in DSC thermograms (see Supporting Information) as well as in X-ray diffractograms (vide infra) of **1P10NO_3**.

Polarized optical micrographs of several of the **1P10A** salts that were cooled from isotropic melts exhibit textures consistent with (but not unique to) layered mesophases (Figure 1).[16] More definitive phase assignments will be derived from X-ray diffraction data. As expected of soft solids, samples of **1P10Cl**, **1P10Br**, and **1P10NO_3** at room temperature retained irregular edges when pressed between cover slips and after the pressure was released; their response to force became more like that of a liquid crystal as the temperature was increased.

The initial micrographs of **1P10Cl·H_2O** and **1P10Br·H_2O** in Figure 1 were obtained without prior heating to avoid loss of water and (partial) conversion to **1P10Cl** and **1P10Br**. Under these conditions, aliquots of both salts were deformable under pressure and their smooth, rounded edges did not return to their original shapes when the pressure was relieved. Lateral force on the cover slips of these liquid-crystalline samples or to **1P10NO_3** above ≈60 °C led to oily streak patterns such as that in Figure 1b. They are consistent with smectic A phases (in which molecules are arranged randomly in layers with their long molecular axes perpendicular to the layer planes) like those reported previously for other **nPmA** salts.[15] The fans in Figures 1a and 1g are not broken, as would be expected of a smectic C phase (structurally related to smectic A phases but with the long molecular axes tilted with respect to the layer planes).[16]

Heats of the transitions leading to isotropic phases are another indicator of whether the phases are solids or liquid crystals. The heats corresponding to transitions to isotropic phases for **1P10Cl·H_2O**, **1P10Br·H_2O**, and **1P10NO_3** (ΔH_{LC-I}) are <3 kJ/mol whereas those for **1P10Cl** and **1P10Br** (ΔH_{K-I}) are ≈10 kJ/mol. Due to the continuous loss of water molecules from **1P10Cl·H_2O** and **1P10Br·H_2O** during heating, their ΔH_{LC-I} values are *upper* limits to those expected for the fully hydrated salts. To obtain the values for the hydrates in Table 1, samples were placed in the DSC chamber at ≈50 °C and heated at 10 °C/min to minimize water loss.

X-ray Diffraction Measurements. The assignment of phase types is based on X-ray diffractograms of the **1P10A** salts and, to a lesser extent, optical micrographs. The diffractograms of the salts in their soft solid phases consist of a strong, narrow, low-angle peak in the range $2\theta = 3.7-4.4°$, higher order diffractions of this peak, several peaks near 15°, and a very broad, weak, high-angle peak at about 20° (Figures 2−6). Diffractograms of liquid-crystalline phases are like those of the soft solids but lack the peaks near 15° and some of the higher order diffractions of the low-angle peak. The progression of the sharp, low-angle peaks is 1, 1/2, 1/3, and so forth, as expected for layered phases.[17] However, some of the higher order reflections are missing in some of the diffractograms. Broad, weak, low-angle peaks at ≈4° in patterns collected at temperatures above the LC/K → isotropic transitions indicate that the isotropic phases of the salts retain some residual lamellar ordering.

On the basis of the broadness and Bragg distance of the high-angle peaks near 20° ($D \approx 4.5$ Å), they are attributed to diffractions from pairs of disordered alkyl chains. The peaks near 15° are assigned to in-plane reflections from charged groups in the ionic planes. They have not been detected previously in diffractions of any other liquid-crystalline **nPmA** salt that we have investigated, although we have sought them. Prior attempts were made with samples in capillaries on diffractometers that are less sensitive than the one employed here or with smeared samples on flat surfaces.[15] The absence of the in-plane reflections in diffractograms recorded on smeared samples *of the soft solids* appears to be due to surface alignments that accentuate 00*l*-type (*hkl*) reflections while attenuating severely the 10*l* type.[18] Although the small number of in-plane reflections makes indexing to a unit cell somewhat uncertain, tentative attributions have been given within the figures. The in-plane diffractions are lost on heating when the solids become liquid-crystalline or isotropic and reappear when the solid phases reform on cooling.

The lamellar spacings (*d*) calculated from the low-angle peaks using Bragg's law[17] are >20 Å, more than the extended length of one **1P10A** molecule (≈15.4 Å),[15] but less than the length of two molecules. The broadness of the high-angle diffraction peaks within the liquid-crystalline phases is inconsistent with smectic phases in which alkyl chains are ordered and, as mentioned above, the optical micrographs are inconsistent with smectic phases with tilted long axes (e.g., smectic C phases, for instance).[19] On these bases, we assign the liquid-crystalline phases to partially interdigitated smectics with long axes orthogonal to the layer planes, smectic A_2 (SmA_2) phases such as those found for other **nPmA** salts (Figure 7).[15,20]

Diffractograms collected on samples of **1P10Cl** and **1P10Cl·H_2O** that had been flame-sealed in glass capillaries included a single low-angle peak at all temperatures (Figures 3 and 4). The diffractogram of **1P10Cl·H_2O** obtained at 60 °C upon cooling from the melt is that of **1P10Cl**; its low-angle peak is at $2\theta = 3.77°$ ($d =$

(16) Demus, D.; Richter, L. *Textures of Liquid Crystals*; VCH: Weinheim, 1978.

(17) Stout, G. H.; Jensen, L. H. *X-ray Structure Determination, A Practical Guide*, 2nd ed.; Wiley: New York, 1989; pp 24, 28.

(18) As demonstrated by the comparative diffractograms in Figures S3−S5 of the Supporting Information, smearing samples on flat surfaces leads to loss of the peaks near 15°.

(19) Demus, D.; Goodby, J.; Gray, G. W.; Spiess, H.-W.; Vill, V. *Handbook of Liquid Crystals, Fundamentals*; Wiley-VCH: New York, 1998; Vol. 1, p 640.

(20) Other packing possibilities are also consistent with the *d*-values. See Figure 10, structures b and c, in ref 15 for two alternatives. We prefer the arrangement in Figure 7 based on our structural studies of *solid* structures of related salts[10] and considerations related to maximization of electrostatic interactions. However, there is no firm evidence that allows us to confirm the model in Figure 7 or eliminate the other possibilities.

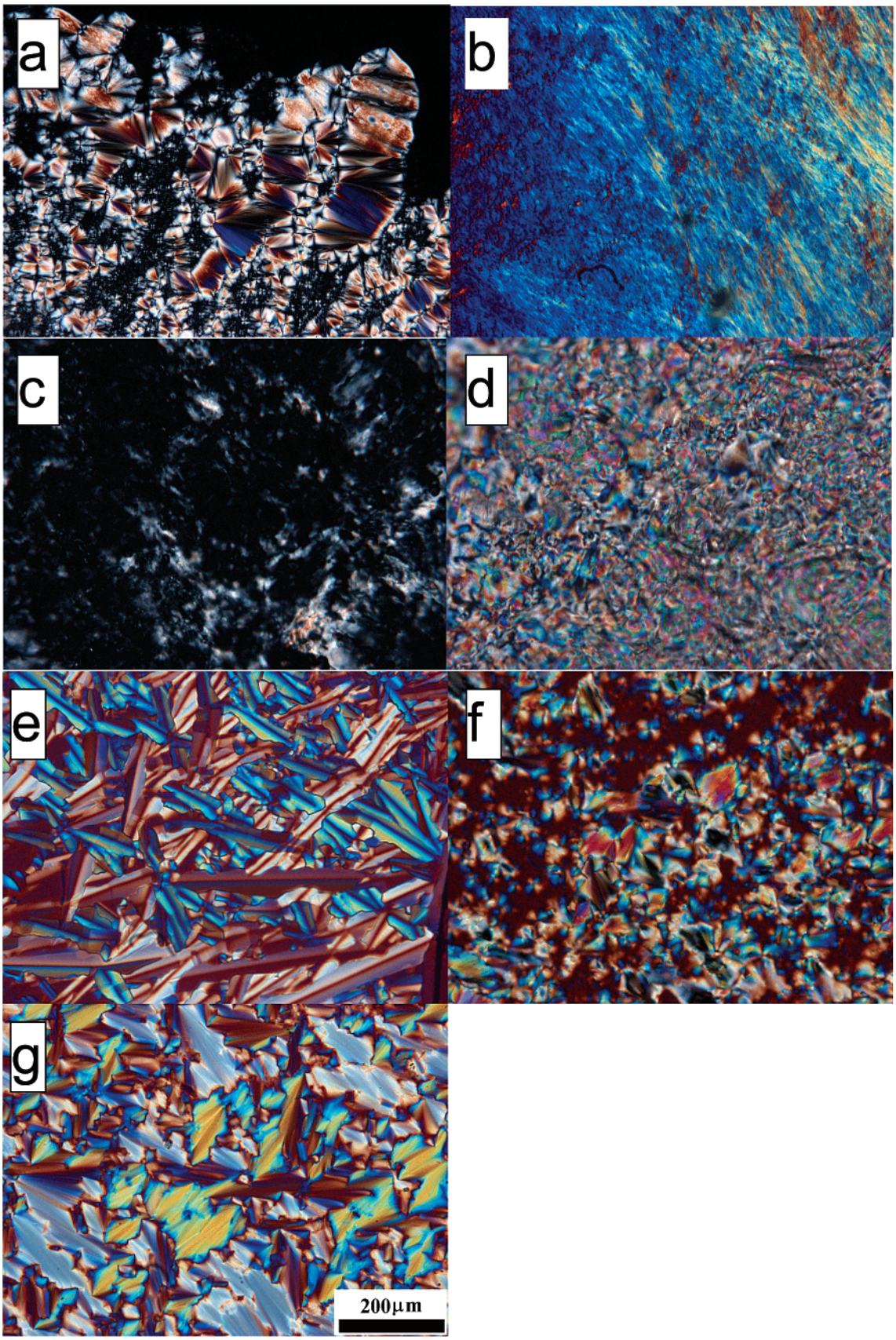

Figure 1. Polarizing optical micrographs of **1P10A** salts at various temperatures. (a) Fanlike texture containing spherulites in **1P10Br·H_2O** at room temperature. (b) Oily streak texture of **1P10Br·H_2O** at room temperature after application of lateral force on the cover slips; the other liquid-crystalline phases give similar patterns when lateral force was applied. (c) **1P10Br** at room temperature. (d) Spherulite texture of **1P10Cl·H_2O** at room temperature. (e) Batonnets forming in a fanlike texture in **1P10Cl** at 40 °C upon cooling. (f) Fanlike texture containing spherulites in **1P10NO_3** at room temperature. (g) Fanlike texture of **1P10NO_3** at 60 °C upon cooling from the isotropic phase. The distance bar in (g) applies to all the micrographs.

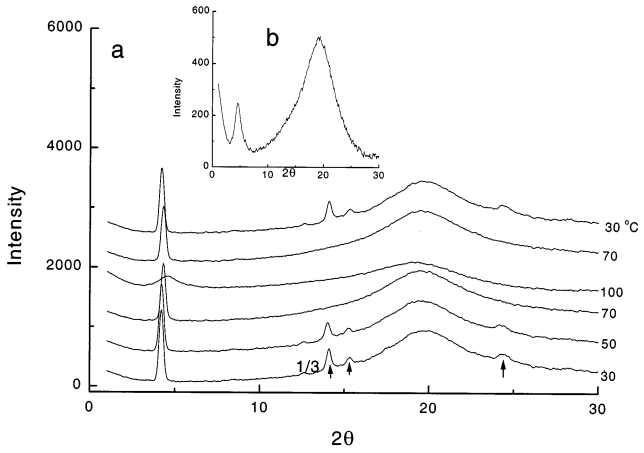

Figure 2. X-ray diffraction patterns of **1P10NO$_3$** at various temperatures measured sequentially from bottom to top (a). The arrows from low angle to high angle indicate peaks ascribed to (001), (−201), and (110) related diffractions (monoclinic), respectively; the other peaks are from 00*l* diffractions and from diffractions associated with the "amorphous" chains; see text for details. (b) Compressed diffraction pattern in the isotropic phase (100 °C); note the residual low-angle peak.

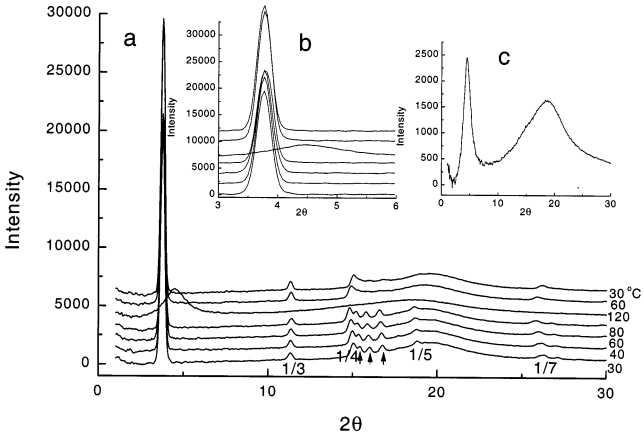

Figure 3. X-ray diffraction patterns of **1P10Cl** at various temperatures measured sequentially from bottom to top (a). The arrows from low angle to high angle indicate peaks ascribed to 10*l* (102, 103, 104) related diffractions (hexagonal). The others are from 00*l* peaks and diffractions associated with the "amorphous" chains; see text for details. (b) Expanded low-angle region of the diffractograms in (a). (c) Compressed diffraction pattern in the isotropic phase (120 °C); note the residual low-angle peak.

23.4 Å), the same position as that of **1P10Cl**, but reverts to $2\theta = 4.06°$ ($d = 21.6$ Å) upon further cooling to 30 °C where, presumably, the water molecules have rehydrated the **1P10Cl**. The relatively sharp peaks in diffractograms of **1P10Cl** (in a sealed capillary) at 30 → 80 °C that are marked by arrows in Figure 3 can be indexed with reasonable probability as distances between 102, 103, or 104 planes in a trigonal (*P*31*c*) cell with unit cell spacings of 6.85 and 46.54 Å. The former distance indicates that the phosphorus atoms of the cationic parts and chloride anions are very well ordered within their ionic layers. It is somewhat larger than the ≲5 Å distance separating adjacent P and Cl atoms within ionic planes of analogous salts in their crystalline phases.[10] When **1P10Cl** was cooled from its (isotropic) melt to the solid phase, the initial diffractograms (60 → 30 °C) lacked the 10*l* peaks, but they reappeared when the samples were incubated for 2 h; the crystal-like arrangement within the ionic layers requires time to anneal organizational defects. These data suggest that alkyl chains are disordered in the soft solid phase of **1P10Cl**, but charged centers constituting the ionic planes are not.

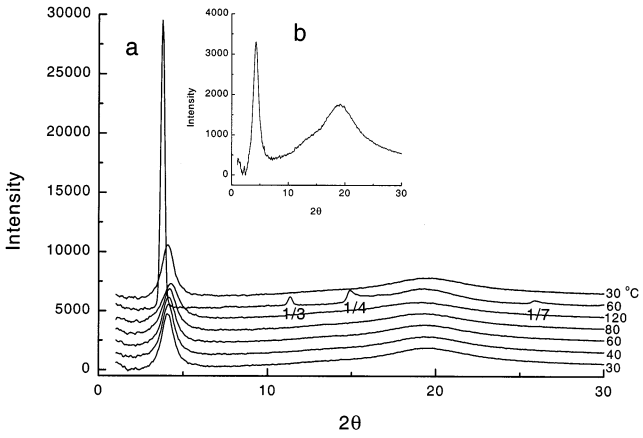

Figure 4. X-ray diffraction patterns of **1P10Cl·H$_2$O** at various temperatures measured sequentially from bottom to top (a). Higher order diffractions of the (001) peak are indicated. (b) Compressed diffraction pattern in the isotropic phase (120 °C); note the residual low-angle peak.

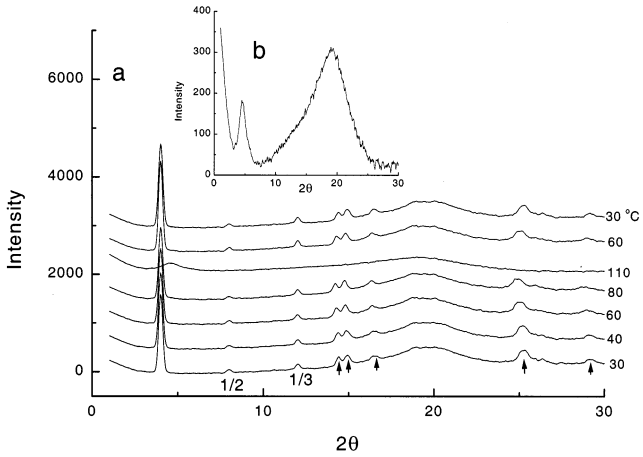

Figure 5. X-ray diffraction patterns of **1P10Br** at various temperatures measured sequentially from bottom to top (a) The arrows from low angle to high angle indicate peaks from (100), (101), (102), (111), and (200) related diffractions (hexagonal), respectively; the other peaks are from 00*l* diffractions and those associated with the "amorphous" chains; see text for details. (b) Compressed diffraction pattern in the isotropic phase (110 °C); note the residual low-angle peak.

The nearly equal layer spacings of **1P10Cl·H$_2$O** and **1P10Cl** and the similarity between their diffraction features and those of the bromide, its hydrate, and the nitrate salts require that the packing of the smectic liquid-crystalline and soft solid phases be similar. The slight differences among the low-angle reflections of the hydrated and nonhydrated forms of one salt, as well as single-crystal X-ray analyses of *tetra*-octadecylphosphonium chloride monohydrate,[10] indicate that water molecules are hydrogen-bonded in the ionic planes that separate the lamellar chains, thereby altering the cross-sectional area occupied by each headgroup.[15]

Measured *d*-values are plotted versus temperature in Figure 8 and presented in Table 2. The layer spacings within the solid phases of **1P10Cl**, **1P10Br**, and **1P10NO$_3$** are independent of temperature. The *d*-

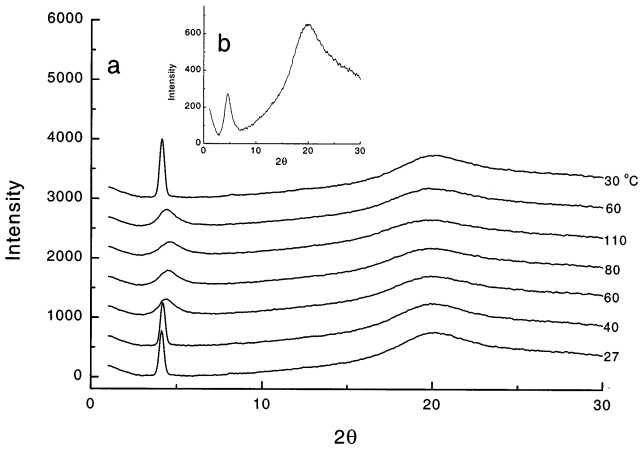

Figure 6. X-ray diffraction patterns of **1P10Br·H_2O** at various temperatures measured sequentially from bottom to top (a). (b) Diffraction pattern in the isotropic phase (110 °C); note the residual low-angle peak.

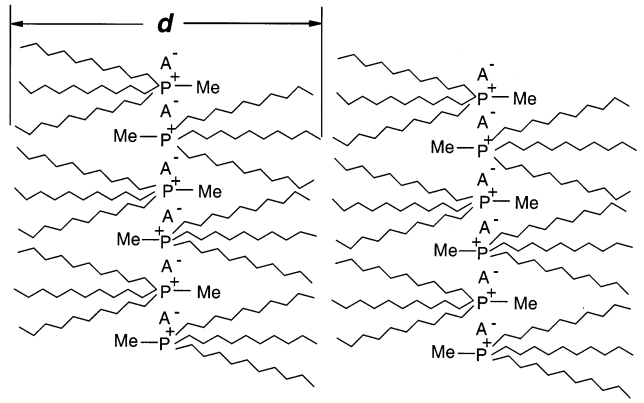

Figure 7. Pictorial representation of the proposed generic packing arrangement of the **1P10A** salts in their layered solid and liquid-crystalline phases. The *n*-alkyl chains form lipophilic layers that are separated by ionic planes composed of the phosphonium headgroups and anions.

spacings of **1P10NO_3** (above its K−LC transition temperature), **1P10Cl·H_2O**, and **1P10Br·H_2O** decrease as the temperature is increased, as expected for a smectic A phase.[21] The *d*-spacings of smectic C mesophases are known to increase with increasing temperature.[21] Within the soft solid phases at a common temperature, 30 °C, **1P10Cl** possesses the largest layer thickness (d = 23.4 Å), followed by **1P10Br** (d = 22.1 Å) and **1P10NO_3** (d = 20.9 Å). This progression may be a result of the strongest ionic interactions being between the phosphonium cation and chloride anions as well as the small size of chloride (compared to bromide and nitrate). Strong ionic interactions lead to more compact ionic planes, less area per *n*-alkyl chain along a layer projection and, consequently, greater chain extension; the cross-sectional area occupied by a phosphonium headgroup and chloride anion within an ionic plane is smaller than the area required by the corresponding groups of **1P10Br** and **1P10NO_3**. Consideration of both

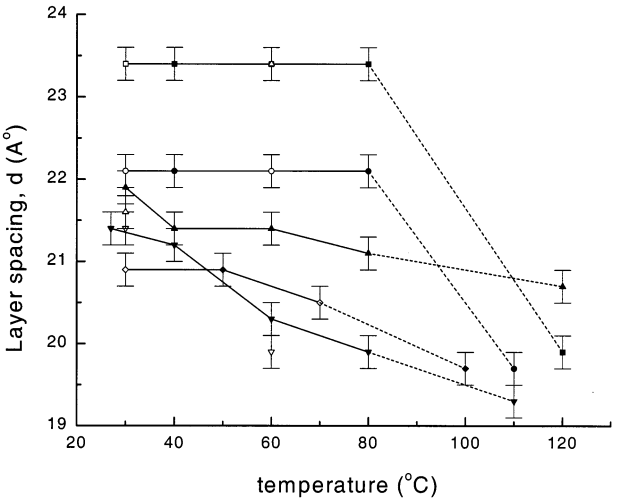

Figure 8. Dependence of the layer spacings on temperature in **1P10A** salts. (□) **1P10Cl**; (○) **1P10Br**; (△) **1P10Cl·H_2O**; (▽) **1P10Br·H_2O**; (◇)**1P10NO_3**. Solid symbols correspond to data obtained on heating to the isotropic phase and open ones to cooling from it. Solid lines connect points within the anisotropic (solid or liquid-crystalline) phases. Dashed lines connect the highest temperature points within the anisotropic phases and the corresponding isotropic phases (points at highest temperature).

Table 2. Measured Layer Thicknesses (*d*);Data Presented in the Order Recorded

1P10NO_3		1P10Cl		1P10Cl·H_2O		1P10Br		1P10Br·H_2O	
temp. (°C)	*d* (Å)	temp. (°C)	*d* (Å)	temp. (°C)	*d* (Å)	temp. (°C)	*d* (Å)	temp. (°C)	*d* (Å)
30	20.9	30	23.4	30	21.9	30	22.1	27	21.4
50	20.9	40	23.4	40	21.4	40	22.1	40	21.2
70	20.5	60	23.4	60	21.4	60	22.1	60	20.3
100	19.7	80	23.4	80	21.1	80	22.1	80	19.9
70	20.5	120	19.9	120	20.7	110	19.7	110	19.3
30	20.9	60	23.4	60	23.4	60	22.1	60	19.9
		30	23.4	30	21.6	27	22.1	30	21.4

factors leads to the same conclusion: the splay angle of the *n*-decyl chains from phosphorus is most restricted in **1P10Cl** and least restricted in **1P10NO_3**, the salt with the largest and most diffusely charged anion. Different ionic interactions and splay angles (controlling London dispersion forces among alkyl chains of one molecule) may also be the principal cause of **1P10Cl** and **1P10Br** being soft solids and their hydrates liquid crystals, the relatively large differences between their transition enthalpies (Table 1), and the differing degrees of ordering within their ionic planes.

Spectroscopic Polarity Measurements. Absorption and emission spectra from Nile Red[22] and 1,1-dicyano-2-[6-(dimethylamino)naphthylen-2-yl]propene (**DDNP**),[23] two solvatochromic dyes, have been used to investigate the polarity of the cybotactic regions within the **1P10A**. The data indicate that these dyes are not within the ionic layers. However, the electronic nature of the dyes must be an important factor in determining their regions of incorporation, and there is no reason to believe that probes of different structure and polarity cannot reside within the ionic layers.[24]

(21) (a) Kumar, S. In *Liquid Crystals*; Kumar, S., Ed.; Cambridge University Press: Cambridge, 2001; pp 10−11, 76−78. (b) Binnemans, K.; Jongen, L.; Bromant, C.; Hinz, D.; Meyer, G. *Inorg. Chem.* **2000**, *39*, 5938. (c) Oriented samples can differentiate smectic A and C phases unambiguously, without relying on optical micrographs.[21a] Unfortunately, we have been unable to orient our **1P10A** salts in capillaries for X-ray analyses. They are easily aligned when smeared on a flat plate, however.

(22) Reichardt, C. *Solvents and Solvent Effects in Organic Chemistry*, 2nd ed.; VCH: Weinheim, 1988; p 359.

(23) Jacobson, A.; Petric, A.; Hogenkamp, D.; Sinur, A.; Barrio, J. R. *J. Am. Chem. Soc.* **1996**, *118*, 5572.

(24) Baker, S. N.; Baker, G. A.; Kane, M. A.; Bright, F. V. *J. Phys. Chem. B* **2001**, *105*, 9663.

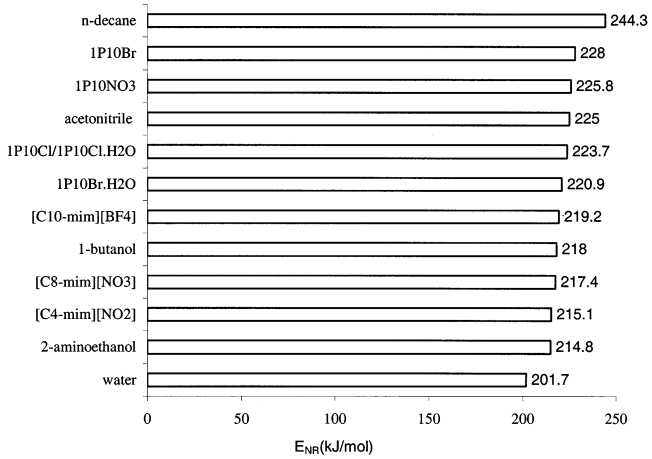

Figure 9. E_{NR} values at room temperature for **1P10A** salts and other media (from literature values[27,28]).

From room-temperature absorption maxima, the average polarity of the environments provided to Nile Red by the salts is in the following order: **1P10Br** < **1P10NO$_3$** < **1P10Cl** ~ **1P10Cl·H$_2$O** < **1P10Br·H$_2$O**.[25] Figure 9 displays the room-temperature molar transition energies[26] (E_{NR}) calculated from the Nile Red absorption maxima (λ_{max}) in the **1P10A** salts, together with the E_{NR} values of several 1-alkyl-3-methylimidazolium ionic liquids (**[C$_n$-mim]X**)[27] and isotropic solvents.[28] According to this probe, the **1P10A**s are less polar than the **[C$_n$-mim]X** ionic liquids for which data are available. Among the nonhydrated **1P10A** salts, the *average* polarities of sites do not correlate with *d* values. From a purely structural standpoint, the smaller the value of *d*, the larger the splay angle of the alkyl chains within a **1P10A** salt and, thus, the greater should be the ability of dye molecules to approach the ionic planes. The splay angle (and, therefore, the ability of a dye molecule to approach the ionic planes) is controlled in large part by the cross-sectional areas of the anions.[15] The polarities sensed by Nile Red in the three salts correlate somewhat with the cross-sectional areas of their anions. We note that residual water that may be present in even carefully dried **1P10Cl** and **1P10Br** samples may affect the proximity of Nile Red molecules to the ionic layers. However, the E_{NR} of a sample of **1P10Cl** that was open to the air for 2 days (to make **1P10Cl·H$_2$O**), 223.7 kJ/mol, is very near that of the "dry" sample; either the water molecules are strongly associated with the **1P10Cl** headgroups, the dye molecules are not very close to the ionic layers, or both. The first hypothesis is supported by the fact that Nile Red reports a much higher polarity in the hydrated bromide salt than in **1P10Br**.

Since absorption maxima in the dry **1P10A** salts were shifted very slightly (usually to higher wavelengths) when the temperature was increased to near the isotropic transitions, the average environments experienced by Nile Red molecules must not change significantly throughout the temperature ranges of the soft solids. For instance, the E_{NR} values of **1P10NO$_3$** were virtually invariant to 90 °C while those of the dry bromide decreased by ≈4 kJ/mol (at 95 °C), and both the chloride *and* hydrated chloride (whose spectra are very similar at each temperature) decreased by only ≈1.6 kJ/mol (at 97 °C); the temperature dependence of Nile Red absorption in **1P10Br·H$_2$O** was not investigated. The largest temperature-induced shift (to *lower* wavelengths), corresponding to an increase in E_{NR} = 5.5 kJ/mol, was observed when Nile Red was heated in an isotropic liquid, 1-butanol, from 5 to 77 °C.

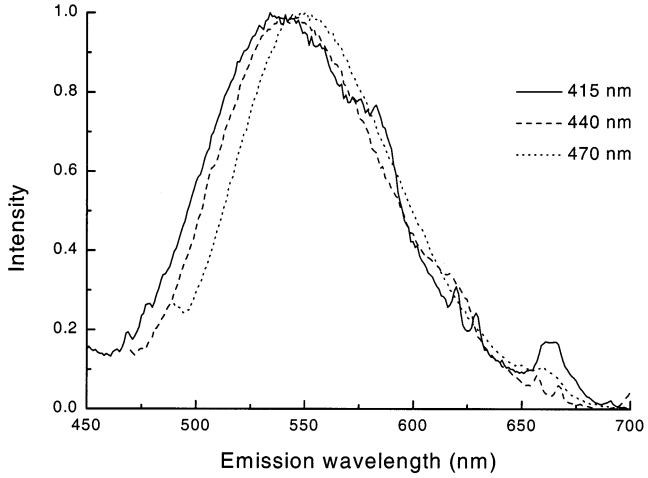

Figure 10. Dependence of the normalized emission spectra of 3.9 × 10^{-4} M **DDNP** in **1P10NO$_3$** at 20 °C on excitation wavelength at the wavelengths indicated.

According to fluorescence measurements,[23] **DDNP** is incorporated somewhat like Nile Red in the **1P10A** solid and liquid-crystalline phases (see Supporting Information for tables of data). At room temperature in **1P10NO$_3$**, the wavelength of maximum emission intensity (λ_{em}) of **DDNP** increased significantly (536 > 548 nm) as the excitation wavelength (λ_{ex}) was increased from 415 to 470 nm (Figure 10). Similar wavelength shifts were noted for the other salts: in **1P10Br**, λ_{em} increased from 533 nm (λ_{ex} = 420 nm) to 545 nm (λ_{ex} = 480 nm); in **1P10Cl**, 556 nm (λ_{ex} = 420 nm) changes to 565 nm (λ_{ex} = 490 nm); in **1P10Cl·H$_2$O**, 548 nm (λ_{ex} = 420 nm) changes to 559 nm (λ_{ex} = 475 nm); in **1P10Br·H$_2$O**, 546 nm (λ_{ex} = 420 nm) changes to 555 nm (λ_{ex} = 475 nm). Because the singlet lifetime of **DDNP** is very short[23] and λ_{em} in CH_2Cl_2 (562 ± 1 nm) and hexane (468 ± 1 nm) was independent of λ_{ex}, we ascribe the wavelength dependencies in the **1P10A** salts to the dye molecules being in sites of different polarities and the magnitudes of the changes in λ_{em} to the breadth of the site distributions. The values of λ_{em} in the **1P10A** indicate an *average* site polarity that is somewhat lower than that afforded by ethanol or acetonitrile (λ_{em} = 600 nm[23]) and higher than that provided by saturated hydrocarbons (λ_{em} ~ 468 nm[23]). Like Nile Red, molecules of **DDNP** do not reside within the region of the ionic headgroups of the **1P10A**.

As the temperature is increased, λ_{em} increases in solid or liquid-crystalline solutions of the **1P10A**. However, **DDNP** appeared to decompose when samples were heated, especially in **1P10NO$_3$** where the fluorescence

(25) Absorption spectra of Nile Red in two conventional solvents, decane and 1-butanol, were in good agreement with published data.[27]

(26) $E_{NR} = (hcN_A/\lambda_{max}) \times 10^6$,[27] where *h* is Planck's constant, *c* is the speed of light, N_A is Avogadro's number, and λ_{max} is the wavelength of maximum absorption (nm).

(27) Carmichael, A. J.; Seddon, K. R. *J. Phys. Org. Chem.* **2000**, *13*, 591.

(28) Deye J. F.; Berger T. A.; Anderson A. G. *Anal. Chem.* **1990**, *62*, 615.

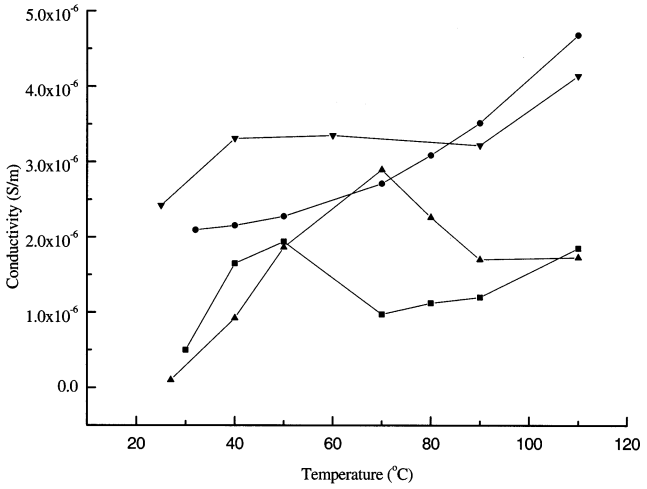

Figure 11. Temperature dependence of the ac conductivity of **1P10A** salts at 20 Hz. (■) **1P10NO3**; (●) **1P10Cl·H2O**; (▲) **1P10Cl**; (▼) **1P10Br**.

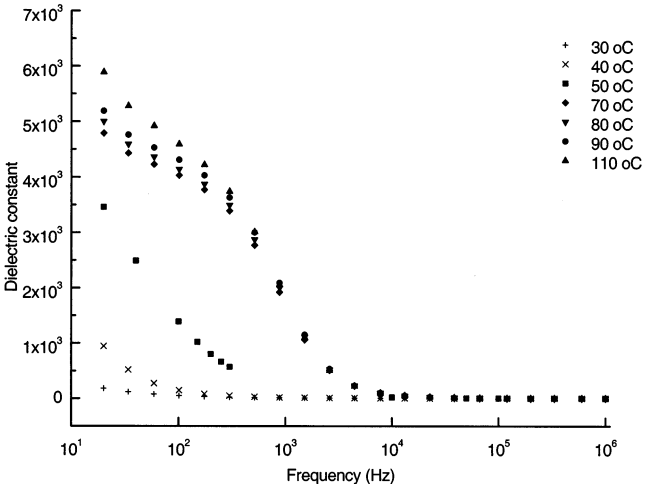

Figure 12. Frequency dependence of the dielectric constant of **1P10NO$_3$** at different temperatures.

spectra of the cooled samples were very different from the ones recorded at high temperature. Significant, irreversible spectral changes were induced by heating **DDNP** in the two hydrates as well. On the basis of the shapes of the fluorescence curves before and after heating, the least thermal decomposition of **DDNP** occurred in **1P10Cl** and **1P10Br**.

Conductivity[29] and Dielectric[30] Measurements. Figure 11 shows the temperature dependence of the ac conductivity of **1P10A** salts at 20 Hz (i.e., near the dc limit).[31] The conductivity of **1P10Cl·H$_2$O** increases regularly with increasing temperature, while that of **1P10Cl** reaches a maximum (2.9×10^{-6} S/m) at 70 °C and then decreases. The conductivity of **1P10Br** is reasonably constant throughout its soft solid temperature range and increases in the isotropic melt where ions become more mobile. The phase transition between the soft solid and smectic phase of **1P10NO$_3$** at 60 °C is discernible in the conductivity measurements. The conductivity rises between 30 and 50 °C, falls at 70 °C, and then rises thereafter. Although detailed interpretations of these data must await further analyses, it is clear that ionic mobility within the phases, whether liquid-crystalline or soft solids, generally increases with increasing temperature.

Although the measured conductivities, $\sim(1-5) \times 10^{-6}$ S m^{-1}, are 10^5-10^6 times smaller than the highest values reported for stable, room-temperature, isotropic ionic liquids,[32] they may be sufficiently large for specific applications, especially if their liquid-crystalline phases can be aligned in the conductance cells. In unaligned samples, conductance is the same (and low) along all laboratory axes because the orientation of planes that are defined by ionic groups changes at the many domain interfaces between electrodes. In aligned samples, conductance along the axis orthogonal to the ionic planes should be exceedingly low because electron or ion flow must pass through the lipophilic regions of the alkyl chains; conductance along any axis within the ionic planes should be exceedingly high because well-organized "salt bridges" span the aligned sample in these directions. Furthermore, if alignment can be modulated, so can conductance.

The frequency dependence of the dielectric constants[30] of the **1P10A** salts, ϵ (the ratio of the capacitance of a filled and empty cell[31]), has also been examined at different temperatures. Data for **1P10NO$_3$** are included in Figure 12. Plots for the other salts are included in Supporting Information. The movement of ions in the low-frequency range (ca. $<10^4$ Hz) results in the dispersions of the dielectric constants.[30] At 20 Hz, ϵ of **1P10Cl·H$_2$O** is larger than that of **1P10Cl** at any temperature compared. This result was expected because of the ion-supporting water molecules in the hydrate. In addition, ϵ of **1P10Br** at 20 Hz is much larger than that of **1P10Cl** at the same temperatures. As noted above, ionic interactions (and, therefore, cationic−anionic associations) are stronger in the chloride than in the bromide salt. The phase transition at 60 °C in **1P10NO$_3$** is clearly manifested in both the shape differences and the magnitudes of the dielectric constants of the 50 and 70 °C data sets plotted in Figure 12. In addition, the frequencies at which the ions are no longer able to follow electric field oscillations[30] for **1P10NO$_3$** at 50 and 70 °C are more different than for any two curves of the other salts separated by 20 °C. The dielectric constants of the **1P10A** salts increase with increasing temperature at the same frequency in the low-frequency range. This is consistent with higher ionic mobilities at higher temperatures.

Summary. The properties of two completely saturated, room-temperature, ionic liquid crystals and three related salts (one of which becomes liquid-crystalline above room temperature) have been characterized by a variety of methods. Optical microscopy and X-ray diffraction experiments indicate that **1P10Cl** and **1P10Br** form soft solid phases, but no liquid-crystalline ones.

(29) (a) Fannin, A. A.; Floreani, D. A.; King, L. A.; Landers, J. S.; Piersma, J. A.; Stech, D. J.; Vaughn, R. L.; Wilkes, J. S.; Williams, J. L. *J. Phys. Chem.* **1983**, *88*, 2614. (b) Schadt, M.; von Planta, C. *J. Chem. Phys.* **1975**, *63*, 4379.

(30) (a) Naemura, S. *J. Soc. Inform. Display* **2000**, *8*, 5. (b) Sawada, A.; Tarumi, K.; Naemura, S. *Jpn. J. Appl. Phys., Pt. 1* **1999**, *38*, 1423. (c) Kalmykov, Yu. P.; Vij, J. K.; Xu, H.; Rappaport, A.; Wand, M. D. *Phys. Rev. E* **1994**, *50*, 2109.

(31) Atkins, P. W. *Physical Chemistry*, 5th ed.; W. H. Freeman: New York, 1994; pp 834, 757.

(32) (a) Bonhôte, P.; Dias, A.-P.; Papageorgiou, N.; Kalyanasundaram, K.; Grätzel, M. *Inorg. Chem.* **1996**, *35*, 1168. (b) Matsumoto, H.; Yanagida, M.; Tanimoto, K.; Nomura, M.; Kitagawa, Y.; Miyazaki, Y. *Chem. Lett.* **2000**, 922. (c) MacFarlane, D. R.; Meakin, P.; Amini, M.; Forsyth, M. *J. Phys.: Condens. Matter* **2001**, *13*, 8257.

However, **1P10NO$_3$** becomes liquid-crystalline at ≈60 °C and **1P10Cl·H$_2$O** and **1P10Br·H$_2$O** are liquid-crystalline at subambient temperatures. All of the salts become isotropic near 100 °C, regardless of whether the lower temperature phase is a soft solid or a liquid crystal. The liquid-crystalline phases are smectic A_2-type (i.e., composed of double layers of *n*-alkyl chains separated by ionic planes); the molecular long axes are orthogonal to the layer planes (as in a smectic A phase). The A-type designation results from the disorganized arrangements of the alkyl chains within a layer, although the positively charged headgroups and their counterions are probably more regularly packed within the ionic planes.

The salts are stable to high temperatures and their liquid-crystalline phases extend over broad temperature ranges. As such, they may be useful as ordered ionic fluids for performing selective transformations of solute molecules[1] or for spectroscopic studies. The conductivities of the salts, whether soft solids or liquid crystals, are much lower than those observed for isotropic ionic liquids due to the attenuated diffusion that is a consequence of molecular ordering and the interruption of long-range electron conduction within the planes described by the ionic centers at domain boundaries. However, the salts may be tunable microcapacitors. Other potential applications for these **1P10A** salts, such as in nonlinear optical generation, even in the absence of external electric fields despite the *bulk* centrosymmetrical packing,[33] are also of interest and will be examined in the future.

Experimental Section

Instrumentation. Thermally induced phase changes were detected by polarizing optical microscopy (Leitz 585 SM-LUX-POL microscope equipped with crossed polars, a Leitz 350 heating stage, and an Omega HH21 Microprocessor thermometer connected to a K/J thermocouple) and differential scanning calorimetry (DSC; TA 2910 DSC cell base interfaced to a TA Thermal Analyst 3100 controller equipped with a hollowed aluminum cooling block into which dry ice was placed for subambient measurements; samples in open aluminum pans under nitrogen atmospheres). X-ray diffractometry was conducted with a Rigaku RAPID/XRD image plate system with Cu Kα X-rays from a Rigaku generator on samples in sealed capillaries. For comparison purposes, some diffractograms were recorded on samples smeared on a flat surface and open to air using a Brucker D8 diffractometer with Cu Kα radiation and an Anton Paar TTK450 camera attachment. Thermal gravimetric analyses (TGA) of salts in platinum pans were performed under a nitrogen atmosphere at a 5 °C/min heating rate on a TA 2050 thermogravimetric analyzer interfaced to a computer.

^{31}P NMR and ^{1}H NMR spectra were recorded on a Varian 300-MHz spectrometer interfaced to a Sparc UNIX computer using Mercury software. Chemical shifts were referenced to external 85% H_3PO_4 (^{31}P) or internal TMS (^{1}H) standards. Absorption spectra were recorded on a Perkin-Elmer Lambda 6 UV/vis spectrometer interfaced to a 386 SX PC with Perkin-Elmer Computerized Spectrometer Software (PECSS). Fluorescence spectra were obtained using a Spex 111 Fluorimeter and a 150-W Xe lamp. The temperature of samples (±1 °C) in both instruments was maintained in a heated cell block and absolute temperatures were calibrated with a thermometer. Elemental analyses were performed by Desert Analytics, Tucson, AZ.

Conductance measurements were performed using an HP 4284A Precision LCR Meter. Samples were introduced by capillary action into 15.7 × 15.7 mm^2 ITO cells with windows separated by uncoated glass cylinders. The precise separations of the cell windows (the average separation was 3.5 μm) were determined from capacitance measurements on the empty cells.[34]

Sample Preparations. Samples for UV/vis and fluorescence measurements were prepared as follows. A 0.3−0.5-mL aliquot of a stock solution of 0.1 mg/mL Nile Red (Aldrich) or 0.85−1.4 mL of a 2.76 × 10^{-4} M **DDNP** (from Dr. Frank Saeva, Kodak Corporation) solution in methylene chloride was transferred to a small test tube. Anhydrous **1P10A** salts (0.5−0.7 mL for Nile Red or 0.6−1.0 mL for **DDNP**) were heated until isotropic and then dissolved in the CH_2Cl_2 solution under a dry N_2 atmosphere. CH_2Cl_2 was removed under vacuum by heating the salts to the temperature at which they began to flow until no more bubbles were observed (≈10 min). Solutions in the hydrated salts were prepared as above except that the samples were allowed to stand for several days in the atmosphere to remove CH_2Cl_2. Nile Red concentrations were (1.2−2.1) × 10^{-4} M and **DDNP** concentrations were 3.9 × 10^{-4} M. Solutions in the anhydrous salts were reheated and transferred to Pyrex cells (0.8-mm path length) that had been purged with N_2 and were then sealed. Solutions in the hydrated salts were smeared onto a quartz disk without heating. Spectra of Nile Red in decane and 1-butanol were recorded also in stoppered Pyrex cells of 2-mm path length. Spectra of **DDNP** in hexane and CH_2Cl_2 were recorded in stoppered Pyrex cells of 0.8-mm path length.

"Dry" **1P10Cl** was prepared by heating samples in a vacuum oven to 140 °C for 3 days. **1P10Cl·H$_2$O** was obtained by leaving samples in the air covered with filter paper for 3 days. Dry **1P10Br** was prepared by placing the salt in a vacuum desiccator beside an open container of P_2O_5 for 2 weeks. **1P10Br·H$_2$O** formed from the dry salt when it was left in a loosely closed container for 1 year.

Syntheses. Similar methods were used to synthesize all of the **1P10A** salts.

1P10Br. tri-Decylphosphine (7.00 g, 15.4 mmol; **TDP**; Cytec Industries, Niagara Falls, Ontario, Canada) was transferred to a round-bottom flask in a glovebox purged with nitrogen. The flask was sealed with a septum and attached via a syringe needle to a Schlenk line purged with nitrogen. Nitrogen was bubbled through 50 mL of chloroform for ≈10 min before being added to the flask by a syringe. Anhydrous bromomethane (2.0 M) in *tert*-butyl methyl ether (8.5 mL, 16.9 mmol) was added, and the solution was stirred continuously for 2 days, initially in an ice bath that was allowed to melt to room temperature. The solution was reduced to a clear oil on a rotary evaporator, recrystallized (3×) from ethyl acetate at −30 °C, and filtered on a Buchner funnel packed in dry ice to afford 6.40 g (76%) of a waxy material, T_{K-I} 97.5 °C. Anal. Calcd for $C_{31}H_{66}PBr$: C, 67.8; H, 12.0; Br, 14.55. Found: C, 67.9; H, 12.41; Br, 14.60. ^{1}H NMR ($CDCl_3$): δ 2.41 (m, 6H), 2.09 (d, J_{P-CH3} 13.5 Hz, 3H), 1.37 (m, 48H), 0.84 (t, J 5.6 Hz, 9H) ppm. ^{31}P NMR ($CDCl_3$): δ 32.17 ppm.

1P10Cl. A mixture of 46.5 mL of 0.187 M methyl-tridecylphosphonium ethyl xanthate[15] (8.7 mmol; **1P10Ex**) in chloroform and 1 mL of 37% hydrochloric acid (12.2 mmol) were stirred in an ice bath that was allowed to melt slowly. After 2 days, the organic layer was washed with HPLC-grade water (3 × 25 mL) and reduced to a yellow oil on a rotary evaporator. The yellow oil was recrystallized (3×) from acetone at −77 °C and filtered on a Buchner funnel packed in dry ice to afford 1.6 g (36.5%) of a deformable, hygroscopic solid. The

(33) Kanazawa, A.; Ikeda, T.; Abe, J. *Angew. Chem., Int. Ed.* **2000**, *39*, 612. The authors argue that second-harmonic generation (SHG) is possible in *macroscopically* centrosymmetric assemblies such as the ones presented here due to *locally* noncentrosymmetric arrangements of pairs of ionic centers within the ionic layers. Applied external electric fields may enhance the polarization and SHG efficiency.

(34) Fishbane, P. M.; Gasiorowicz, S.; Thornton, S. T. *Physics for Scientists and Engineers*, 2nd ed.; Prentice Hall: New Jersey, 1996; p 699.

solid was stored under vacuum next to P_2O_5 for 4 days prior to characterization: T_{K-I} 96.2 °C. Anal. Calcd for $C_{31}H_{66}PCl$: C, 73.69; H, 13.17; Cl, 7.02. Found: C, 73.36; H, 13.55; Cl, 6.72. ^1H NMR ($CDCl_3$): δ 2.41 (m, 6H), 2.10 (d, J_{P-CH3} 13.2 Hz, 3H), 1.5 (s, 48H), 0.88 (t, J 6.6 Hz, 9H) ppm. ^{31}P NMR ($CDCl_3$): δ 32.32 ppm.

1P10NO$_3$. A mixture of 100 mL of 0.467 M **1P10Ex**[15] (46.68 mmol) in chloroform and 3 mL (70%, 53.94 mmol) of nitric acid were stirred in an ice bath that was allowed to melt slowly. After 2 days, the organic layer was washed with HPLC-grade water (3 × 50 mL) and reduced to a yellow oil on a rotary evaporator. The yellow oil was recrystallized (3×) from acetone at −77 °C and filtered on a Buchner funnel packed in dry ice to afford 14.22 g (57.3%) of a deformable white solid, T_{SmA2-I} 74.4 °C. Anal. Calcd for $C_{31}H_{66}PNO_3$: C, 70.01; H, 12.51; N, 2.63. Found: C, 70.25; H, 12.59; N, 2.23. ^1H NMR ($CDCl_3$): δ 2.3 (m, 6H), 1.95 (d, J_{P-CH3} 13.6 Hz, 3H), 1.3 (s, 48H), 0.88 (t, J 6.6 Hz, 9H) ppm. ^{31}P NMR ($CDCl_3$): δ 32.3 ppm.

Acknowledgment. We are extremely grateful to Dr. Al Robertson of Cytec Corporation for preparing and donating tri-*n*-decylphosphine, to Dr. Frank Saeva of Kodak for a sample of **DDNP** and bringing this molecule to our attention, to Prof. Vaclav Horak for interesting discussions, to Prof. Bryan Eichorn and Dr. Kannadka Ramesh of the University of Maryland for allowing us to repeat some of the X-ray measurements, and to the National Science Foundation and the Petroleum Research Fund (administered by the American Chemical Society) for financial support. We also acknowledge several very useful suggestions and comments of the referees.

Supporting Information Available: Six tables of fluorescence data for **DDNP** in CH_2Cl_2, hexane, and **1P10A** salts, two figures of DSC thermograms for **1P10Cl·H$_2$O** and **1P10NO$_3$**, three figures comparing the X-ray diffraction patterns of **1P10A** salts obtained from a Bruker D8 diffractometer and a Rigaku Rapid diffractometer at room temperature, and three figures showing the frequency dependence of the dielectric constant of **1P10Br**, **1P10Cl**, and **1P10Cl·H$_2$O** at different temperatures (PDF). This material is available free of charge via the Internet at http://pubs.acs.org.

CM010930X